Composites: Part B 68 (2015) 392–400

Contents lists available at ScienceDirect

Composites: Part B

journal homepage: www.elsevier.com/locate/compositesb

Impact of perlite, vermiculite and cement on the thermal conductivity of a plaster composite material: Experimental and numerical approaches

S. Abidi [a,*], B. Nait-Ali [b], Y. Joliff [c], C. Favotto [a]

[a] Université de Toulon, CNRS, IM2NP, UMR 7334, 83957 La Garde, France
[b] GEMH (EA 3178), Ecole Nationale Supérieure de Céramique Industrielle, 12 rue Atlantis, 87068 Limoges Cedex, France
[c] Université de Toulon, MAPIEM, EA 4323, 83957 La Garde, France

ARTICLE INFO

Article history:
Received 7 April 2014
Received in revised form 21 July 2014
Accepted 25 July 2014
Available online 16 September 2014

Keywords:
A. Ceramic–matrix composites (CMCs)
B. Thermal properties
C. Finite element analysis (FEA)

ABSTRACT

This work is dealing with the thermo mechanical behaviour of a new composite material used as thermal insulator and for fire passive protection in building construction. The composite panel results of combination of a calcium sulphate hydrates matrix mainly water and inorganic mineral additives. The effective thermal conductivity of the composite is measured by the hot-disc method. Analytical and numerical models are used to determine the composite thermal conductivity which can be expected vs the rate of additives. The experimental values are compared with analytical and numerical models. In particular, effective medium percolation theory (EMPT) for a two-phase system gives analytical values which are close to the experimental results. Moreover, the numerical model based on a simple description can allow the description of the thermal conductivity evolution with the rate of additives. An unexpected phenomenon which can be attributed to the confined water in additives can explain the gap between the numerical models and the experimental results.

1. Introduction

The introduction of more restrictive standards (environmental materials, energy consumption, fire protection, etc.) in building construction leads to develop new materials [1–6]. The material must have good properties as thermal insulator in standard condition and moreover it will be used as a fire protection for construction building. Materials usually used are based on inorganic compounds as concrete or gypsum [7–11]. The main advantages of gypsum are its availability, its low cost, its ease of production and its quality as fire barrier. Indeed, when gypsum is subjected to fire, the endothermic dehydration process consumes a part of fire energy. Nevertheless, the main disadvantage of plaster is its brittleness at room temperature and its poor resistance to crack opening and propagation when it is subjected to fire conditions as described in the standard curve ISO 834 [12]. So, to enhance the fire resistance of the material and to improve its insulator properties, additives are usually introduced in the gypsum matrix. For fire protection, the additives usually used are vermiculite, mica, alumina, perlite, ceramic hollow sphere [30,31].

One particular class of these materials is constituted by materials containing a large volume fraction of porosity which are used in situations requiring very good thermal insulation [13]. The prediction of their thermal properties and especially the effective thermal conductivity by analytical or numerical models is therefore of strong interest [14,15]. Collishaw and Evans [16] have reviewed some analytical expressions for the calculation of the effective thermal conductivity of a porous solid. In each case, the expression is based on a geometrical simplification of the microstructure concerning the spatial distribution of the porous phases in the matrix. The pertinence of this approximation to the real microstructure determines the validity of a chosen model. For materials containing small amounts of porosity (<20%), the prediction of the thermal conductivity is less critical than for highly porous materials. This study deals with the influence of the microstructure on the effective thermal conductivity for materials containing from 45% to 75% porosity through experimental measurements, analytical and numerical calculations. These materials are essentially based on an inorganic matrix of predominantly calcium sulphate dihydrate, $CaSO_4{\cdot}2H_2O$, and additives used as thermal and mechanical reinforcements.

2. Materials and methods

2.1. Matrix materials

The composites developed are based on industrial gypsum matrix (Algiss). The particles size distribution of the plaster is

---

* Corresponding author.
E-mail address: abidi@univ-tln.fr (S. Abidi).

http://dx.doi.org/10.1016/j.compositesb.2014.07.030
1359-8368/© 2014 Elsevier Ltd. All rights reserved.

measured by laser diffraction and shows a repartition in volume: 2/3 around 10 μm and 1/3 around 150 μm (Fig. 1).

The Scanning electron microscopy (SEM) observation (Fig. 2) of the plaster shows a flaky structure characteristic of β-hemihydrates [1] and a large crystal which could be residual dehydrate after the incomplete dehydration of dehydrate extracted from quarries. To determine the different species present in the plaster, thermo gravimetric and differential thermal analysis (TGA and DTA) analysis have been realized.

The mass loss and the heat flux as a function of temperature are determined by running a TGA 92 of Setaram under air flow starting at 25 °C and going up to 1200 °C at a heating rate of 10 °C min^{-1}. A blank is realized with an empty alumina crucible of 100 mL before each measure. Four measures are realized with around 50 mg of plaster to verify the reproducibility of the measures. The DTA–TGA curves on Fig. 3 show the different stages of dehydration of the industrial plaster (see Figs. 4–6).

Around 150 °C, the mass loss Δm1 associated with the endothermic peak 1 is a feature of the departure of 3/2 mol of H_2O from dehydrate (Eq. (1)). This result shows the presence of dihydrate as impurity in the industrial plaster [21].

$$CaSO_4, 2H_2O \rightarrow CaSO_4, 1/2H_2O_{(di)} + 3/2H_2O \qquad (1)$$

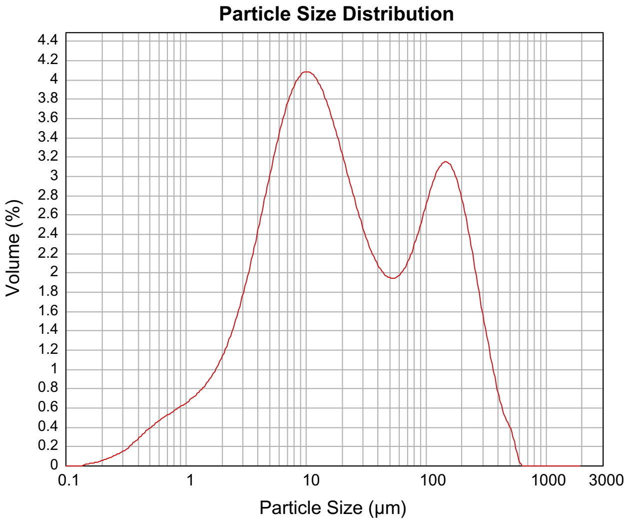

Fig. 1. Particles size distribution of the plaster matrix (laser diffraction measurements).

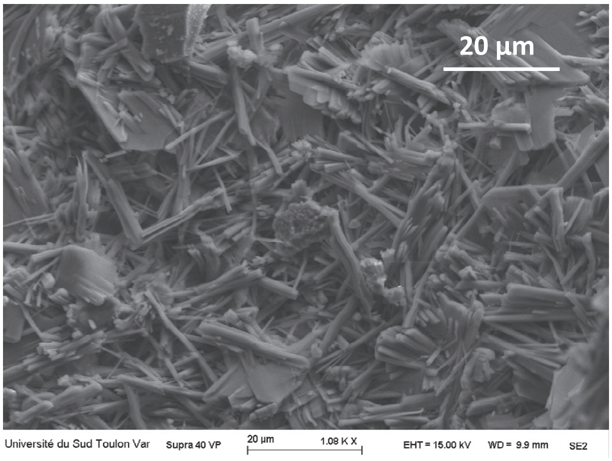

Fig. 2. SEM observation of the plaster matrix.

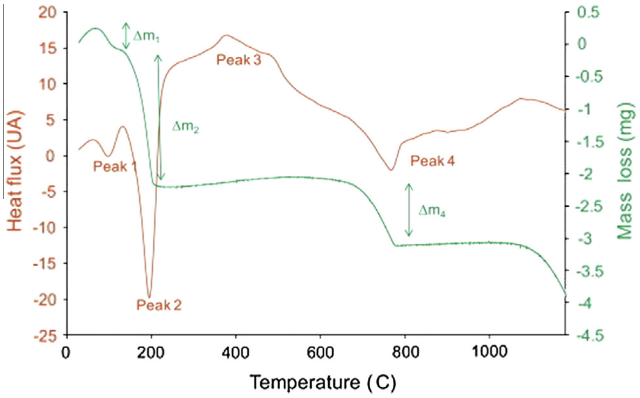

Fig. 3. DTA–TGA curves obtained with the industrial plaster Algiss.

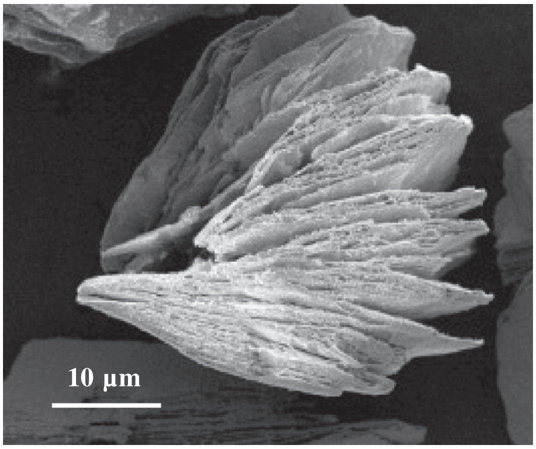

Fig. 4. SEM observation of the exfoliated vermiculite (GRANUTEC® E).

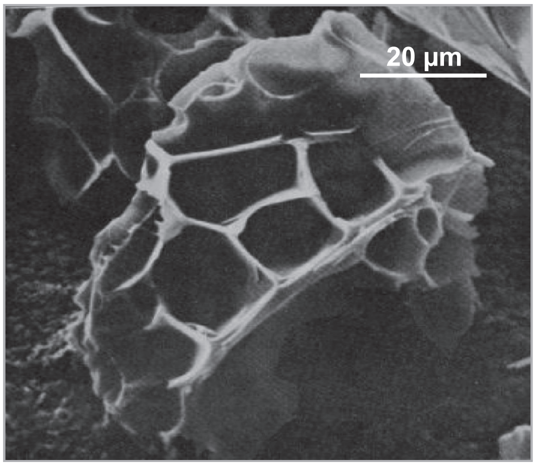

Fig. 5. SEM observation of the perlite (P10).

At 200 °C, the mass loss Δm2 associated with the endothermic peak 2 corresponds to the departure of 1/2 mol of H_2O from the hemihydrate obtained after the incomplete dehydration of dihydrate and from the β-hemihydrate of plaster (Eqs. (2) and (3)).

$$CaSO_4, 1/2H_2O(di) \rightarrow CaSO_4 + 1/2H_2O \qquad (2)$$

$$CaSO_4, 1/2H_2O(\beta) \rightarrow CaSO_4 + 1/2H_2O \qquad (3)$$